

Optimal control technique applied to the minimization of uncertainty measurements in surveying instruments

Achille Germain Feumo¹ , Jean François Wounba²,
André Talla³ and Gervis Roméo Tueguem S⁴

Measurement and Control
1–11

© The Author(s) 2024

Article reuse guidelines:

sagepub.com/journals-permissions

DOI: 10.1177/00202940241259907

journals.sagepub.com/home/mac



Abstract

The objective of this study was to develop an optimal control approach by numerical calculus to predict how to reduce the overall uncertainty of survey instruments unable to directly measure inaccessible points. To reach our goal, two approaches were used to attain the objective. The first was inspired by mathematical models related to three methods appropriately selected and contained in Zhuo's work proposed in 2012. These were Remote Elevation Measurement (REM), Remote Elevation Dual Measurement (REDM), and Front-to-Back Measurement (FBM) methods whose uncertainties on the measurements of points were deduced using error propagation equations. Optimal control technique helps us to show that for the REM, the height h of the prism contributed more than 70% compared to the global uncertainty for ranges $S < 50m$ from the prism. For the REDM, when the distance between two consecutive stations increases, the weight of the contribution of the two zenith angles z_1 and z_2 tends to 50% each for z_1 close to z_2 , which is to be avoided. For the FBM, the weight of the contribution during the front measurement process before is negligible. The second approach used the Swedish regulation of SIS-TS 21 143:2009 which classified total stations according to types of uncertainty to compare the results given by the total station of class T3 unable to directly measure inaccessible points with the more sophisticated class T1 station with direct measurements. Thus, for small spans at the rear measurements $S_{DG} = 10m$, the height h_2 of the front prism has the greatest relative contribution more than 90% for zenithal differences $z_1 - z_2 = 40gon$. This results of our analysis were convincing and provided designers with the data to minimize the overall uncertainties essential in the conception of total stations.

Keywords

Total station, inaccessible points, uncertainty, propagation of uncertainties, optimal control

Date received: 26 December 2023; accepted: 17 May 2024

Introduction

The analysis of the contribution weight of the relative importance of each component of the overall uncertainty is essential to identifying the sources of uncertainty that can be addressed potentially, to reduce the overall uncertainty. Measurements in industries have become more important in view of the fact that, measurements provide the basis for any control. The management of random errors associated with any indirect measurement problem is a major concern in the field of surveying and even in all other areas of science. Surveying refers to the science of accurately measuring horizontal and/or vertical distances in the field. There are many surveying problems that can occur during the process: instrument errors caused by incorrect calibration or incorrect use of instruments; environmental

factors such as wind, rain, or fog can distort or block the survey signal; human error where surveyors can

¹Department of Mathematics, University of Yaounde I, Yaounde, Cameroon

²Department of Civil Engineering, University of Yaounde I, Yaounde, Cameroon

³Department of Mechanic, University of Yaounde I, Yaounde, Cameroon

⁴Department of Physic, University of Yaounde I, Yaounde, Cameroon

Data Availability Statement included at the end of the article

André Talla is now affiliated to Department of Environment, National Advanced School of Public Works, Yaounde, Cameroon.

Corresponding author:

Achille Germain Feumo, Department of Mathematics, University of Yaounde I, box 510 yaounde, Yaounde, Cameroon.

Email: aafeumo@gmail.com



Creative Commons CC BY: This article is distributed under the terms of the Creative Commons Attribution 4.0 License (<https://creativecommons.org/licenses/by/4.0/>) which permits any use, reproduction and distribution of the work without

further permission provided the original work is attributed as specified on the SAGE and Open Access pages (<https://us.sagepub.com/en-us/nam/open-access-at-sage>).

make mistakes in taking measurements or in reading the instruments (see Idoje et al¹ and Hussein et al.²). The reduction of errors due to the total station when measuring the vertical angle is a major problem in improving the accuracy of trigonometric leveling. The most popular techniques for identifying and analyzing sources of the overall uncertainty are developed in engineering literature such as the models which included the uncertainty in the sample's mass and of the volumetric glassware (confere Harvey³ and Cheng et al.⁴)

Thus, Zhou and Sun⁵ proposes the method of leveling combining the total station with a tracking bar to reduce the sources of errors of trigonometric leveling. On the other hand, Ghilani and Wolf⁶ analyzing the individual sizes contributes to functional error when measuring the elevation of a point. The combined standard uncertainty evaluation is performed and the uncertainties of azimuth and elevation angles are established and the system's measurement accuracy is also calculated.⁷ Nowadays, the coefficient of contribution to uncertainty plays an important role in the development of tools and the choice of electronic instruments such as total stations and GPS, that it allowed⁸ to propose the coefficient of contribution to the uncertainty that is appropriate for the correlated and uncorrelated input variables. This allowed them to improve the procedure for determining the molar mass of lead and its uncertainty from the four isotopes of lead.

The three methods developed in this work have already been addressed by.⁷ But the analysis of the weight of the individual contribution to the overall uncertainty needed to identify the parameters responsible for the rapid growth of the overall random error had not yet been made. Knowledge of the contribution of each of these parameters in the measurement of inaccessible points by applying one of the methods highlighted with less efficient equipment makes it possible to equal the result. The originality of this work lies in the fact that we performed numerical simulations of the weight of the individual contribution to global uncertainty and the law of propagation of uncertainties. This offers us a huge opportunity to find ways and means to improve the measurement process for the three methods. In addition, the geometric configurations associated with trigonometric methods play a very important role in the quality of the data obtained during the measurement processes. Surveyors always choose the most appropriate equipment such as total station which is capable of scanning interfaces through a cloud of points based on the control point and back sight and simulation process. For example, the T1 class total station is highly expensive piece of equipment than the T3 class total station. In light of this assertion that numerical simulations have an important role to play in probing the different configurations that can allow us to improve the measurement process, this allows us to be more efficient and to save cost and time in the end.

We assume that systematic errors are reduced during the measurement process. Then, only the random errors obey the law of propagation of the uncertainties. The

purpose here is to study the effects of the propagation of random errors in an indirect measurement process and give appropriate recommendations for each method. To meet our defined objective, a numerical analysis is performed with the MATLAB software tool (R2019 a, win 64). The theory of these methods is presented and the theoretical uncertainty of each method is deduced and analyzed numerically. Then, the measurement of uncertainty is evaluated. In addition, some recommendations on methods are given. Using these indirect methods, the altitudes above the ground of inaccessible points can be measured with less risk and less effort, which will eventually save time and increase efficiency.

This paper is organized as follows: Section 2 presents the mathematical models of three methods. A brief classification of total stations according to the standard and the measurement of uncertainty for different class total stations are presented. Section 3 is devoted to analyzing the sources of errors and proposing error reduction strategy which is the core of this work. Our results ended up with a discussion and a conclusion.

Methodology

Many different techniques can be used to measure data quantities such as heights, plane coordinates, vertical and horizontal angles, horizontal and inclined distances. Numerous instruments and methods have been developed for this purpose. It is almost impossible to take observations in the surveying process that are completely stable; which means free from small variations caused by errors. With these error-prone measured data, it's a matter of establishing their effects on the measurements. This involves starting from the indirect measurements and determining its mathematical relationship to evaluate its direct measurement.

The methodological approach used in this study (see Trélat⁹) is that of an optimal control problem consisting of two parts: determining an optimal trajectory (distance, height, angle) joining an initial set (indirect measurements) to a target (minimizing overall uncertainty), and ascertaining that the target is attainable with reference to Zhuo's⁷ various methods. Next, numerical simulations will help us to better calibrate our instruments in order to assess its optimal trajectory.

The typical measurement propagation law for a quantity U as a function of independent measurements x_1, x_2, \dots, x_n where $U = f(x_1, x_2, \dots, x_n)$ is given by:

$$S_U^2 = \sum_{i=1}^n \left(\frac{\partial U}{\partial x_i} \right)^2 S_{x_i}^2 \quad (1)$$

where S_U is the standard error of U and are standard errors of x_1, x_2, \dots, x_n respectively.

Remote elevation measurement (REM) method

The principle of the REM (see Duggal¹⁰) is illustrated in Figure 1 below:

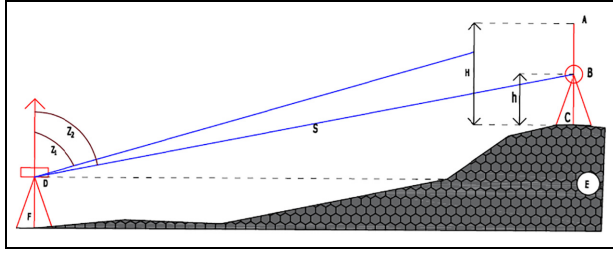


Figure 1. Schematic diagram of the REM, where the zenith distances z_1, z_2 are measured by a total station in D (confere Zhuo⁷).

where a prism B is vertically positioned under an unknown point A , the height h of the prism ground is measured and the distance from the slope to the prism from a remote position such as F , is determined by a total station D as well as the two zenith distances z_1, z_2 . The height H above ground is found by trigonometry:

$$H = S \sin(z_2) \cotan(z_1) - S \cos(z_2) + h \quad (2)$$

The standard uncertainty of the REM associated with height H above the ground is obtained according to JCGM 100¹¹ by the formula (1) of the combined standard uncertainty which can be written as

$$u_H^2 = \sum_{i=1}^4 c_i^2 u^2(x_i) \text{ with } c_i = \frac{\partial H}{\partial x_i} \quad (3)$$

This is the law of propagation of uncertainties (see Zhang and Wang¹²), where c_i is the sensitivity coefficient of the input estimate $x_i = S_i, z_i, h_i$ (S_i is the tilt distance of the prism between two points, z_i is the zenith angle, and h_i the height). It is important to note that we assume that the input estimate x_i is not correlated.

$$u_H^2 = (\sin(z_2) \cotan(z_1) - \cos(z_2))^2 u^2(S) + \frac{S^2 \sin^2(z_2)}{\sin^4(z_1)} u^2(z_1) + S^2 (\cos(z_2) \cotan(z_1) + \sin(z_2))^2 u^2(z_2) + u^2(h) \quad (4)$$

At this level, it may be useful to analyze the relative importance of each component of uncertainty. For this, we defined relative contribution coefficients:

$$R_i \approx \frac{\left(\frac{\partial H}{\partial x_i}\right)^2 u^2(x_i)}{u_H^2} \quad (5)$$

This is the eigenvalue contribution of the error variance (uncertainty square) on x_i with respect to the total error variance. This calculation of relative importance is a useful tool for identifying sources of uncertainty that can be addressed to reduce overall uncertainty.

The uncertainty analysis provides a formal and systematic framework for quantifying the uncertainty

associated with system results. In addition, it provides the designer with useful information on the contribution of each stochastic fundamental parameter to the overall uncertainty of system outputs. This knowledge is essential for identifying the “important” parameters that need to be given more attention, in order to better evaluate their values and thereby reduce the overall uncertainty of the system results. When a system involves basic parameters whose values cannot be certain, the traditional approach is to perform a sensitivity analysis to quantify the rate of change of the output of the model, due to a change of unit in a basic parameter.

In the equation (5), the individual terms $\left(\frac{\partial H}{\partial x_i}\right)^2 u^2(x_i)$ represent the individual contribution to the total error, resulting from the observation errors in each independent variable. When the size of the error estimated by a function is too large, the inspection of these individual terms will indicate the most important contributors to the error. The most effective way to reduce the overall error in function is to look closely at how to reduce the most important error terms in equation (4).

All electronically measured distance observations (confere Ceylan¹³) are subjected to instrumental errors that manufacturers consider to be a constant error a and a scalar error b . A typical specified precision is $\pm(a + b \text{ ppm})$. In this expression, generally $1 \leq a \leq 10 \text{ mm}$ and b generally ranges from 1 to 10 parts per million (ppm). Other errors involved in electronically measured distance observations come from centering errors of the target and the instrument. Given that, in any survey involving multiple stations, the estimated random error (confere Ghilani and Wolf¹⁴) in an observed distance is:

$$u(S) = \pm \sqrt{\sigma_i^2 + \sigma_r^2 + a^2 + (Sb \text{ ppm})^2} \quad (6)$$

Where $\sigma_i = 1.5 \text{ mm}$ is the centering error of the instrument height 1.5 m which is not negligible in the context of the measurement method used because the total station is moved then stationed during the operations of measure and $\sigma_r = 1 \text{ mm}$ is the centering error of the reflector. It should be noted that the prism cannot change position during the measurement process. For the total station, the estimated error for a single observation (see Ghilani and Wolf¹⁴) of zenith angles is:

$$u(z) = \pm \sqrt{(2 \times \sigma_{ISO}^2 + \sigma_B^2)} \quad (7)$$

where σ_{ISO} is the ISO 17123-3 standard for the instrument and σ_B the error in the vertical compensator or in the leveling of the circular bubble. The values of σ_{ISO} , and $(a + b \text{ ppm}) = 2 + 2 \text{ ppm}$ are contained in the classification table of total stations according to the standard SIS-TS 21,143 used. Thus, an analysis of the coefficient of relative importance with a class T3 (TCR 403) total station is given in Figure 2 below by using equation (5).

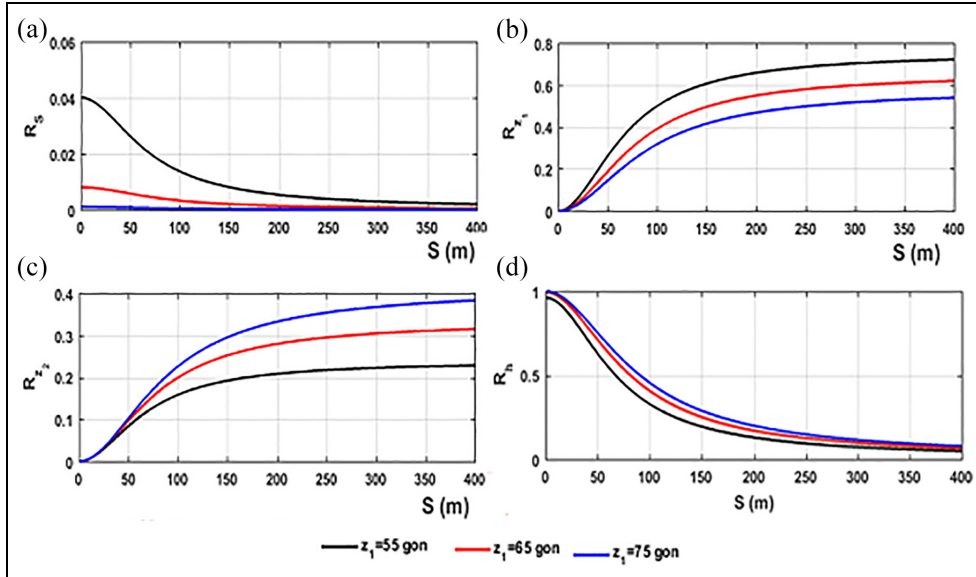


Figure 2. Analysis of the relative importance of each component of global uncertainty for class T3 total station: R_S , R_{z_1} , R_{z_2} , and R_h for figures (a), (b), (c), and (d) respectively where $z_2 = 102 \text{ gon}$, $u(z_1) = u(z_2) = u(z)$ and $u(S) = u(h)$.

In this case, the equation (4) reads:

$$u_H^2 = \left(1 + \frac{\sin^2(z_2 - z_1)}{\sin^2(z_1)}\right) u^2(z) + S^2 \left(\frac{\sin^2(z_2)}{\sin^4(z_1)} + \frac{\cos^2(z_2 - z_1)}{\sin^2(z_1)}\right) u^2(h) \quad (8)$$

For $z_2 = 102 \text{ gon}$, the uncertainty component of z_1 is dominant at more than 60% and the uncertainty component of z_2 at more than 30% for stations located more than 150 m from the reflector. Thus, at more than 150 m, it is advisable to use precise angle devices by performing repetitive measurements on z_1 and z_2 to act on the overall uncertainty. In other words, $u(z_1)$ and $u(z_2)$ must be small for long-range configurations with respect to the reflector. On the other hand, stations within 20 m of the reflector will have the uncertainty component on the reflector's height, gradually increased to more than 90% of the contribution to overall uncertainty. Hence, there is a need to act using extremely precise devices in such distances. As z_1 increases, the contributions of S and z_1 to the overall uncertainty decrease, while those of the parameters h and z_2 increase.

The tachymeter used to collect data in this study is a Leica TCR 403 total station with an angular precision of 1 mm gon and a distance precision of 2 mm + 2 ppm. The data to determine the numerical measurement uncertainty of the methods presented have been collected from a Swedish regulation called SIS-TS 21143: 2009 (see Cederholm and Jensen¹⁵).

In this regulation, total stations have been classified as read in Table 1 below according to the expected standard uncertainties, with the aim of predicting the distances and zenith angles to measure, to obtain the

Table 1. Classification of total stations according to the SIS-TS 21143: 2009 standard.

Class	Standard uncertainty in direction $u(\text{dir})$	Standard uncertainty in distance $u(d)$
T_1	0.2 mgon	1 mm + 2 ppm
T_2	0.6 mgon	3 mm + 3 ppm
T_3	1 mgon	3 mm + 3 ppm

Table 2. Measurement uncertainty for class T3 total stations as a function of S for the REM method ($z_2 = 102 \text{ gon}$).

	Class T3 total stations					
	3.3	3.5	4.5	6.1	7.8	10.5
$u_H(\text{mm})$	20	35	100	150	200	300
$S(\text{m})$	85	60	100	75	72	83
$z_1(\text{gon})$						

lowest possible overall uncertainty of the object to measure.

Table 2 below shows the values of the uncertainties under the influence of the parameters z_1 and S .

The simultaneous effects of the main parameters of influence z_1 and S on the overall uncertainty are represented in Figure 3, with $\sigma_B = 0.3 \text{ mgon}$ and $\sigma_{ISO} = 1 \text{ mgon}$.

The overall uncertainty increases rapidly as the stationing distance S relative to the reflector increases. On the other hand, the influence that a class T1 (TM6100A) total station can have on global uncertainty is studied. To do this, the observations are recorded and illustrated in Table 3, highlighting an increase in the level of accuracy on a class T1 with $\sigma_B = 0.15 \text{ mgon}$, $\sigma_{ISO} = 0.15 \text{ mgon}$ and $(a + b \text{ ppm}) = 1 + 2 \text{ ppm}$ Where

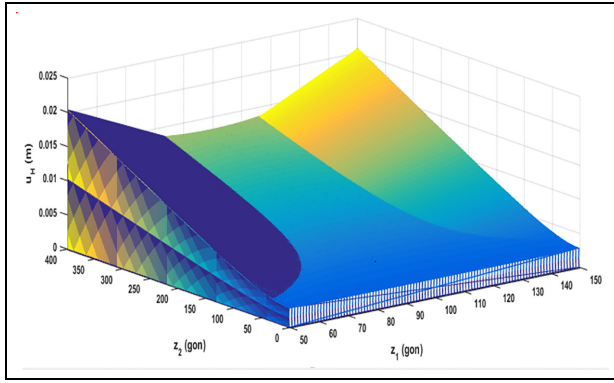


Figure 3. Global uncertainty analysis for class T3 total stations according to parameters S and z_1 ($z_2 = 102$ gon).

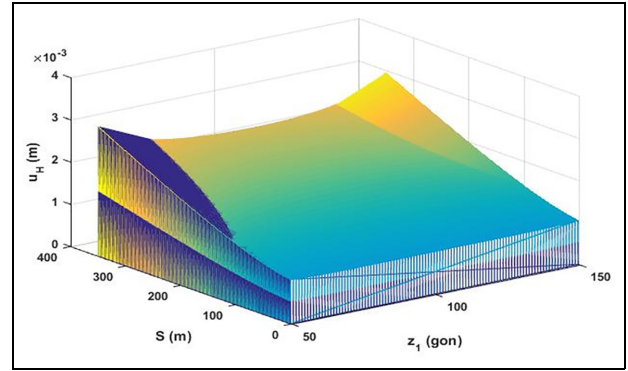


Figure 4. Analysis of the overall uncertainty for a class T1 total station according to parameters S and z_1 ; ($z_2 = 102$ gon).

Table 3. Measurement uncertainty as a function of S and z_1 for the REM method ($z_2 = 102$ gon).

	Class T1 total stations					
u_H (mm)	2.7	2.7	2.8	2.9	3	3.3
S (m)	20	35	100	150	200	300
z_1 (gon)	85	60	100	75	72	83

$\sigma_i = 1mm$ is the centering error of the instrument height 1.5 m, $\sigma_r = 1mm$ is the centering error of the reflector.

A graphical representation of the uncertainty as a function of parameters z_1 and S is carried out in Figure 4.

Moreover, for a fixed value of the global uncertainty on the height $u_H = 3mm$ fixed, it is possible to find a maximum value of the positioning distance S beyond which this prediction cannot be achieved. This value of u_H given, allows us to solve the parameter S function of z_1 and z_2 using equation (8) and Figure 5 below is obtained with the class T3 total station.

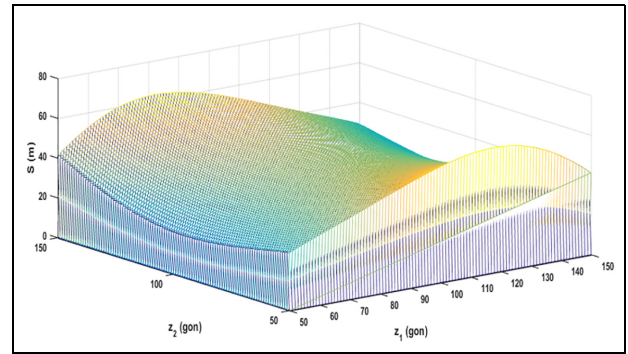


Figure 5. Highlighting the maximum positioning distance for a class T3 total station, knowing that $u_H = 3mm$.

Remote elevation dual measurement (REDM) method

The principle of the REDM is illustrated in Figure 6.

Heights H_1 and H_2 above the ground are measured using the REM. As seen in Figure 6, when a prism is positioned at point F and a total station at point O_1 , zenith distance z_1 at unknown point A is measured with a total station at O_1 . The total station can be moved to point O_2 where point O_2 is closer to the unknown point A , and the zenith distance z_2 to unknown point A is measured by a total station at point O_2 . H_3 which is the difference in height between points E and F , can be measured with a leveling instrument. Finally, the height H above the ground can be calculated using trigonometry function. Note that the value $(H_1 - H_2)$ can be positive or negative; when it is negative, the unknown point A is below the prism in F , the point C is also below the point D and the value $(H_1 - H_2)$ is therefore negative.

Thus, the height above ground H of the unknown point inaccessible A is:

$$H = H_1 + (H_1 - H_2) \frac{\cos(z_1)\sin(z_2)}{\sin(z_1 - z_2)} - H_3 \quad (9)$$

Recall formula (1), the explicit form of the combined standard uncertainty of height H above ground of unknown point A inaccessible reads:

$$u_H^2 = \frac{(H_1 - H_2)^2}{\sin^4(z_1 - z_2)} [\cos^2(z_2)\sin^2(z_2)u^2(z_1) + \cos^2(z_1)\sin^2(z_1)u^2(z_2)] + \left[1 + \frac{\cos(z_1)\sin(z_2)}{\sin(z_1 - z_2)}\right]^2 u^2(H_1) + \frac{\cos^2(z_1)\sin^2(z_2)}{\sin^2(z_1 - z_2)} u^2(H_2) + u^2(H_3) \quad (10)$$

It is important to identify the parameters that a small variation will induce a rapid increase in overall uncertainty. A graphical representation of the relative importance of each component of the uncertainty resulting from the equation (5) allows to obtain Figure 7.

Generally, when $H_1 - H_2$ grows, it means that the distance between two consecutive sets increases as well.

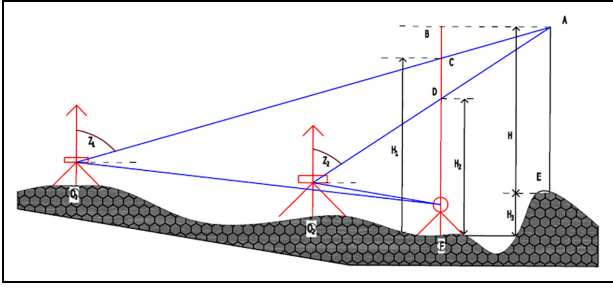


Figure 6. Diagram of the principle of the REDM method (conferre Zhuo⁷).

For this purpose, Figure 7 shows an overall increase in the relative contribution weight of the parameters z_1 and z_2 ; on the other hand, an overall decrease in the relative contribution weight of the H_1 , H_2 and H_3 .

Thus, for values of $|z_1 - z_2| \geq 10 \text{ gon}$, the contribution weight of the angles z_1 and z_2 tends to zero, and the overall uncertainty is dominated by the contribution weight of the parameters H_1 and H_2 . Especially, when $z_1 - z_2 = 20 \text{ gon}$, the dominant contribution weight parameter is R_{H_1} , when H_2 and H_3 have a negligible contribution. In this case, the use of extremely precise devices at a distance is recommended. On the other hand, a zenith difference such that $|z_1 - z_2| \leq 10 \text{ gon}$ (with z_1 different of z_2) will see an exponential increase in the weight of the contribution of the angles z_1 and z_2 while that of the other parameters decreases to zero. This case is to be avoided because the precision of the devices is limited. The standard uncertainty formula gives a clear indication of the adverse situation that might occur in cases where the difference between the two measured zenith distances is small. In order to measure the simultaneous effects that the major parameters $H_1 - H_2$ and $z_1 - z_2$ may have on the uncertainty u_H , the observations are recorded in Table 4 and represented in Figure 8.

Thus, the increase in the difference $H_1 - H_2$ results in a growth of uncertainty u_H . This situation corresponds to the increase of the distance separating the two consecutive positions of setting O_1 and O_2 in the case of a relative at the ground. On the other hand, a zenithal difference $z_1 - z_2$ tending toward zero will increase the uncertainty u_H exponentially. The overall uncertainty increases rapidly when the difference $z_1 - z_2$ tends to 0 gon ; so, a low value of $z_1 - z_2$ is to be avoided. But in the case where $H_1 - H_2$ is large, it will always be necessary to be reassured that $z_1 - z_2$ is not close to zero because the uncertainty is extremely sensitive to the zenith difference $z_1 - z_2$. In addition, in the case of measurements made with class T1 measuring instruments, the influence of the measurement parameters on the uncertainty is illustrated in Table 5 and shown in Figure 9.

A marked improvement in uncertainty is observed because the uncertainties obtained with a class T1 total station are more accurate than those obtained with a

class T3 total station. The class of the total station has an important influence on the overall uncertainty of the height to be measured. Among the largest accuracies, we can expect an accuracy of 2.2 mm with a class T1 total station. On the other hand, with the total station of class T3, a precision of 3.1 mm can be reached. Thus, the expected results with the class T3 total station are less accurate than those obtained with a class T1 total station.

The front-to-back measurement (FBM) method

The principle of the FBM method is shown in Figure 10 below,

where a total station is placed at point M and its height h_1 is measured above the ground with a measuring tape, we observe the unknown point A by measuring the zenith distance z_1 . The total station is replaced by a prism at point M , and the height of the prism is adjusted so that it is equal to h_1 . The total station is moved to point K which is closer to the inaccessible area. The unknown point A is again observed by measuring the zenithal distance z_2 . Then, another N prism is placed at point J . The zenith distances z_3 and z_4 are measured by the total station in G .

Thus, the height H above the ground of the unknown point inaccessible A reads:

$$H = \frac{S_{DG} \cos(z_1) \sin(z_2 + z_4)}{\sin(z_1 - z_2)} + S_{DG} \cos(z_4) + S_{GN} \cos(z_3) + h_2 \quad (11)$$

where S_{DG} is the tilt distance of the prism between point D and point G . The standard uncertainty of the height H above the ground of the unknown point A inaccessible reads:

$$\begin{aligned} u_H^2 & \left(S_{DG} \sin(z_2 + z_4) \frac{\cos(z_2)}{\sin^2(z_1 - z_2)} \right)^2 u^2(z_1) \\ & + \left(S_{DG} \cos(z_1) \frac{\sin(z_1 + z_4)}{\sin^2(z_1 - z_2)} \right)^2 u^2(z_2) \\ & + (S_{DG} \sin(z_3))^2 u^2(z_3) \\ & + S_{DG}^2 \left[\cos(z_1) \frac{\cos(z_2 + z_4)}{\sin(z_1 - z_2)} - \sin(z_4) \right]^2 u^2(z_4) \\ & + \left[\cos(z_1) \frac{\sin(z_2 + z_4)}{\sin(z_1 - z_2)} + \cos(z_4) \right]^2 u^2(S_{DG}) \\ & + \cos^2(z_3) u^2(S_{GN}) + u^2(h_2) \end{aligned} \quad (12)$$

Equation (12) is a very complex functional relationship giving uncertainty as a function of indirect measurement parameters. It is therefore, important to analyze the weight of the relative importance of the specific contributions to the angle and distance parameters in relation to the overall uncertainty. Thus, the

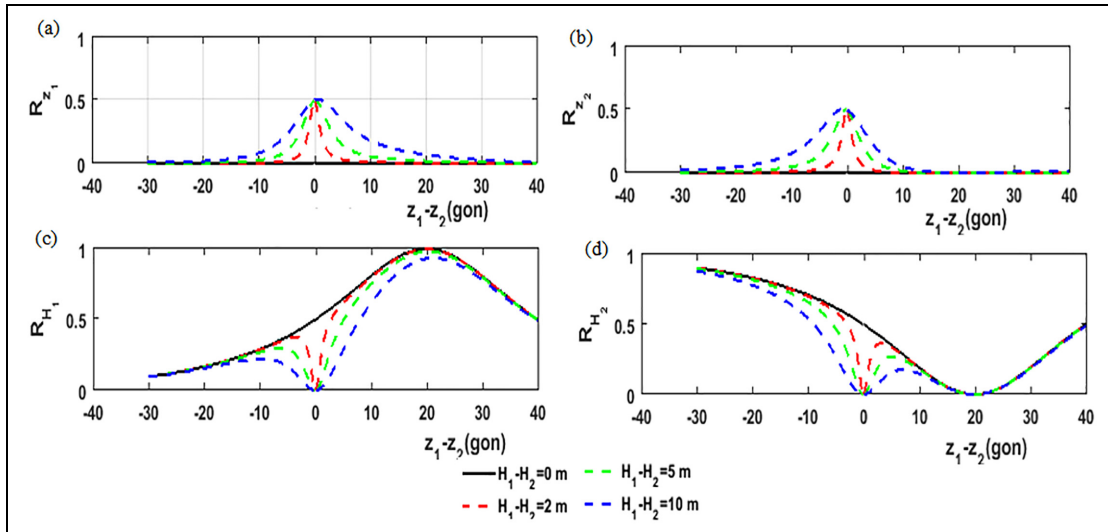


Figure 7. Analysis of the relative importance of each component of the global uncertainty for class T3 total station: R_{Z_1} , R_{Z_2} , R_{H_1} , and R_{H_2} for figures (a), (b), (c), and (d) respectively where ($z_2 = 80$ gon).

Table 4. Measurement uncertainty as a function of $H_1 - H_2$ and $z_1 - z_2$ for the REDM method ($z_2 = 90$ gon).

Class T3 total stations						
$u_H(mm)$	4.6	5	36.6	3.5	3.1	3.7
$H_1 - H_2(m)$	-5	-1.5	0	1.1	1.5	5
$z_1 - z_2(gon)$	-20	-15	-1	10	15	23

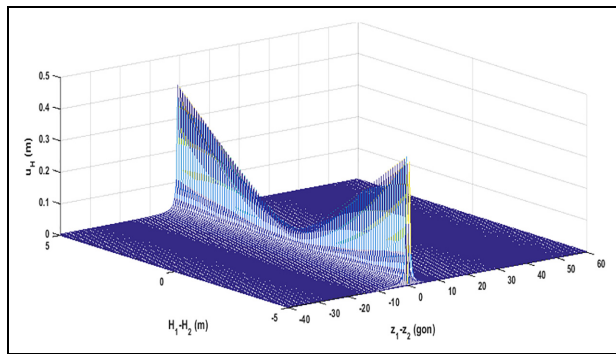


Figure 8. Variation for a class T3 total station of the global uncertainty as a function of $H_1 - H_2$ and $z_1 - z_2$; ($z_2 = 90$ gon).

Table 5. Measurement uncertainty as a function of $H_1 - H_2$ and $z_1 - z_2$ for the REDM method ($z_2 = 90$ gon).

Class T1 total stations						
$u_H(mm)$	3.3	3.6	26.7	2.6	2.2	2.2
$H_1 - H_2(m)$	-5	-1.5	0	1.1	1.5	5
$z_1 - z_2(gon)$	-20	-15	-1	10	15	23

weight of the different sources of parameter errors is shown in Figure 11 below:

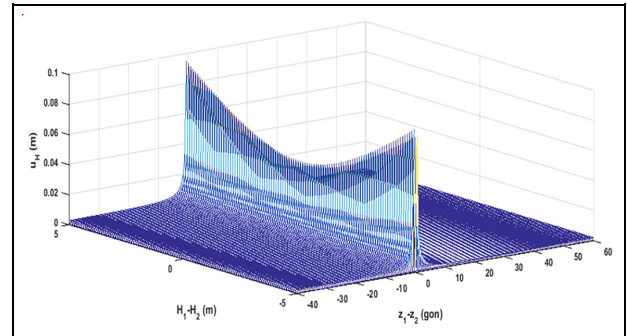


Figure 9. Variation for a class T1 total station of the overall uncertainty as a function of $H_1 - H_2$ and $z_1 - z_2$, ($z_2 = 90$ gon).

When the distance S_{DG} increases, the weight of the relative contribution associated with the parameters z_1 , z_2 and z_4 increases given respectively by Figure 11(a), (b), and (d) while the weight of the contribution of the parameters z_3 , S_{DG} , h and S_{GN} decreases conferred respectively by Figure 11(c) and (e)–(g). Thus, for large rear spans, it is important to use a highly accurate total angle station. Moreover, a small weight of the relative contribution during the front sight S_{GN} and a relative contribution associated with S_{DG} can be noted to reach 50% of the global uncertainty for $|z_1 - z_2| = 10$ gon with $S_{DG} = 10m$. On the other hand, for zenith angle differences $z_1 - z_2 > 20$ gon, the extreme accuracy in determining the height of the prism is necessary to reduce the overall uncertainty. Subsequently, a small variation in the uncertainty for the two total station classes as a function of the front sight characterized by the S_{GN} distance is illustrated in Table 6 and shown in Figure 12 as follows:

The overall uncertainty u_H varies slightly to within for distances ranging from 1.7 to 300m for a T1 class total station. On the other hand, for a total station of

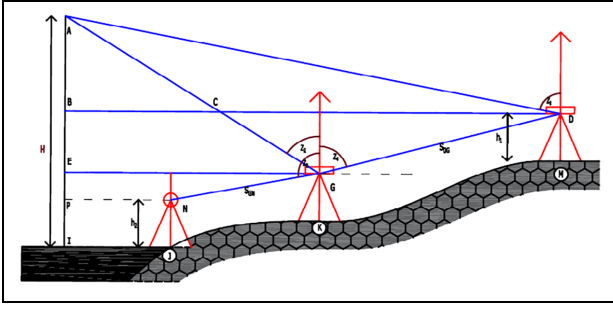


Figure 10. Diagram of the principle of the FBM method (confere Zhuo⁷).

class T1, the uncertainty varies to the millimeter under the same conditions.

However, the influence of the backsight characterized by the S_{DG} distance on the overall uncertainty is illustrated in Figure 13

Uncertainty strongly increase with S_{DG} . Thus, the rear sight contributes greatly to the increase of the global uncertainty u_H for long ranges S_{DG} because as shown in Figure 13, a rear range of 300 m can generate an uncertainty of more than 40 mm for class T3 total station and 6.4 mm for class T1 total station. In order to measure the simultaneous effects that the major parameters S_{DG} and $z_1 - z_2$ may have on the uncertainty u_H , Figure 13 is shown.

Moreover, Figure 14 above shows that the overall uncertainty u_H increases rapidly as a function of the distance S_{DG} which separates the total station and the prism placed at the rear. But this situation can be corrected if the difference of zenith angles is at least greater than 10 gon. Thus, in a practical setting, even when the reflector placed at the rear is away from the total station, it must be ensured that the difference of zenith angles is not close to zero for the effect of compensation of the uncertainties to be possible.

Results and discussion

In this work, the numerical simulations are performed in a context where the spans separating the prism of the instrument cannot go beyond 300 m. This has neglected the refraction of light and the effect of the roundness of the earth (see¹⁴). Thus, a good measure of the weight of the contribution of a component of the uncertainty must be without dimension such as $R_i \in [0, 1]$ (0%–100%). In Figure 2, globally, one realizes that for $z_2 = 102$ gon, with z_1 increasing, the weights R_S and R_{z_1} decrease as those of R_{z_2} and R_h increase. Thus, for $S \leq 30$ m the weight of the individual contribution of the prism $R_h \geq 80\%$ of the global uncertainty with z_1 increasing from 55 gon. Likewise, for increasing the tilt distance of the prism S, the weights R_{z_1} and R_{z_2} increase and their

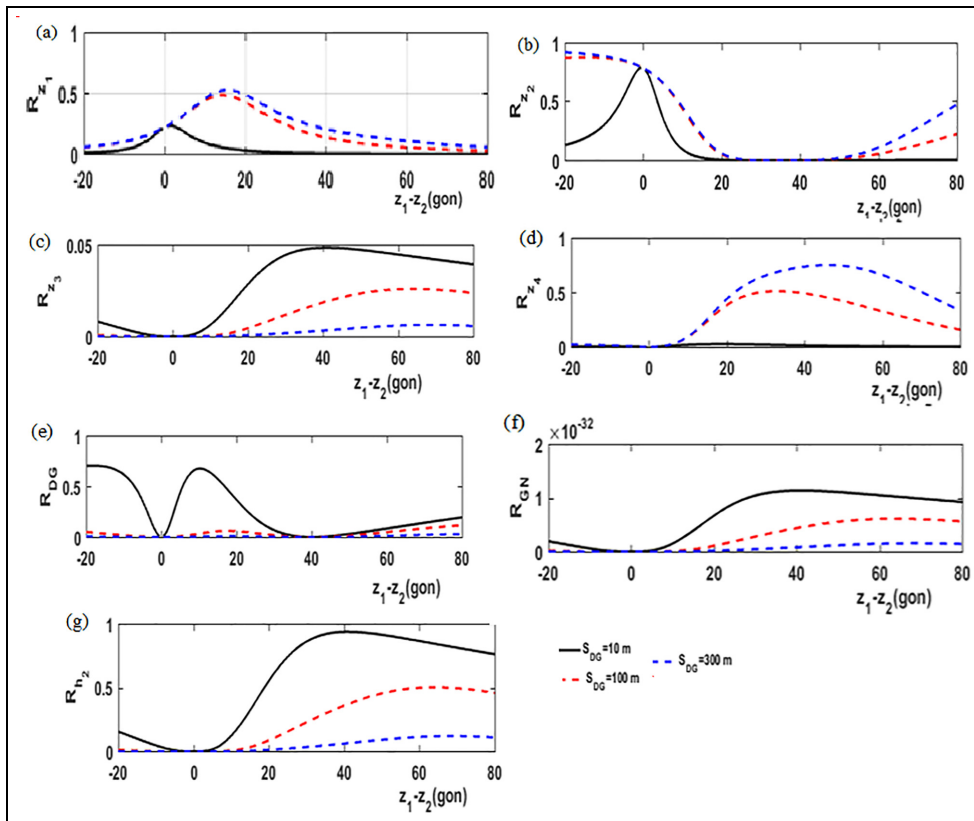


Figure 11. Analysis of the relative importance of each component of global uncertainty for class T3 total station: R_{z_1} , R_{z_2} , R_{z_3} , R_{z_4} , $R_{DG} = R_{S_{DG}}$, $R_{CN} = R_{S_{GN}}$, and R_{h_2} for figures (a), (b), (c), (d), (e), (f), and (g) respectively where ($S_{GN} = 15$ m, $z_2 = 70$ gon, $z_3 = 110$ gon, $z_4 = 80$ gon).

Table 6. Slight variation of overall uncertainty as a function of S_{GN} for class T3 for the FBM method.

Class T3 total stations							
$u_H(mm)$	4.5	5.6	144.5	452.8	6.6	5.1	5
$S_{DG}(m)$	5	10	7	15	15	19	20
$z_1 - z_2(gon)$	-20	-12	-1	1	8	10.5	12.5

effects can be reduced by using a total station of high angular precision, that is to say, low values of u_H .

Figure 4 shows a clear improvement in the accuracy due to the characteristics of the class T1 total station compared to that of T3 obtained in Figure 3. The theory of the REM method is simple, but the observation process is a bit more complex, because when positioning the prism under the unknown point, the prism should be placed very close to the vertical area below or above the unknown point. Which is not always obvious in the field.

Moreover, the REDM is influenced by weights of R_{z_1} and R_{z_2} when z_1 is close to z_2 , which is to be avoided. Thus, $R_{z_1} + R_{z_2}$ tends toward 100% of the contribution to global uncertainty while the other contributions are of negligible weight. On the other hand, for $z_1 - z_2 = 20gon$ the weight of the contribution of R_{H_1} tends toward 100% for H_1 close to H_2 and the contribution of R_{H_3} is negligible. Indeed, when $H_1 - H_2$ increases, the contribution weights of R_{z_1} and R_{z_2} increase as R_{H_1} , R_{H_2} , and R_{H_3} decrease. Thus, an increase in $H_1 - H_2$ corresponds to an increase of distance O_1O_2 on a relatively flat ground, that is to a large difference in elevation between two consecutive stations O_1 and O_2 on a rough terrain. Figure 7 illustrates the fact that it is important to avoid that $z_1 - z_2$ tends to zero. The disadvantage of the REDM method is that it is necessary to place a total station at two positions, the process then becomes a little more complex than for the

REM. The use of the method has the advantage of being able to position a prism at any location, not necessarily under the plumb line of unknown points, the method could be widely used in surveying work.

On the other hand, the FBM is influenced by weights of R_{z_1} and R_{z_2} when z_1 is close to z_2 , which is to be avoided. Moreover, R_{z_1} , R_{z_2} and R_{z_3} and R_{z_4} increase with S_{DG} while R_{z_3} , R_{z_2} and R_{GN} , R_{DG} decrease. Thus, backsighting corresponds to the determination of the AGD triangle which greatly increases the overall level of uncertainty while the forward ones have a very small influence on the overall level of uncertainty. This is perfectly illustrated by Figures 11–13. The front-to-back measurement method can be used to determine the height of objects above, for example in water areas; compared to the REM and the REDM, this method is more flexible when choosing the position of the prisms. The disadvantage of this method is that the rear prism is removed from the tripod to be replaced by the total station at each operation. This can introduce errors during measurements.

Conclusion

The class T3 total station used as a survey instrument in this paper with appropriate method selected, gave us results as precise and convincing as much as would have given the total station of higher class T1 more powerful and 10 times more expensive. Thus, analysis of numerical simulations of the overall uncertainty of point measurement using a given method depends on the contribution affecting it, not the tool. For this reason, the optimal control technique informs us that the displacement altitude measurement method produces better height accuracy for points where it is possible to place a prism under the plumb line; whereas the double distance altitude measurement method is recommended, since in this case the prism can be placed at

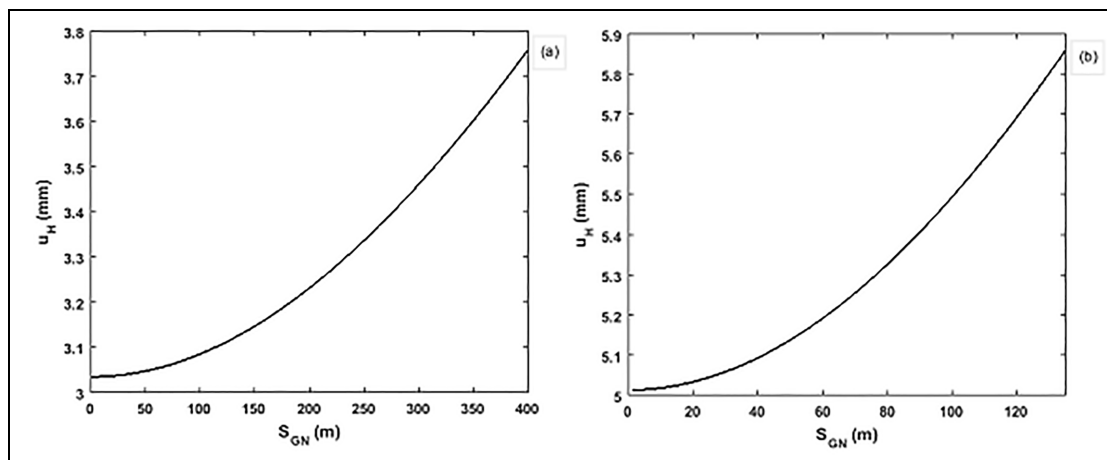


Figure 12. Slight variation of overall uncertainty as a function of S_{GN} for class T1 and T3 total stations respectively for Figures (a) and (b); ($z_1 = 80gon$, $z_2 = 70gon$, $z_3 = 100gon$, $z_4 = 90gon$, $S_{DG} = 15m$).

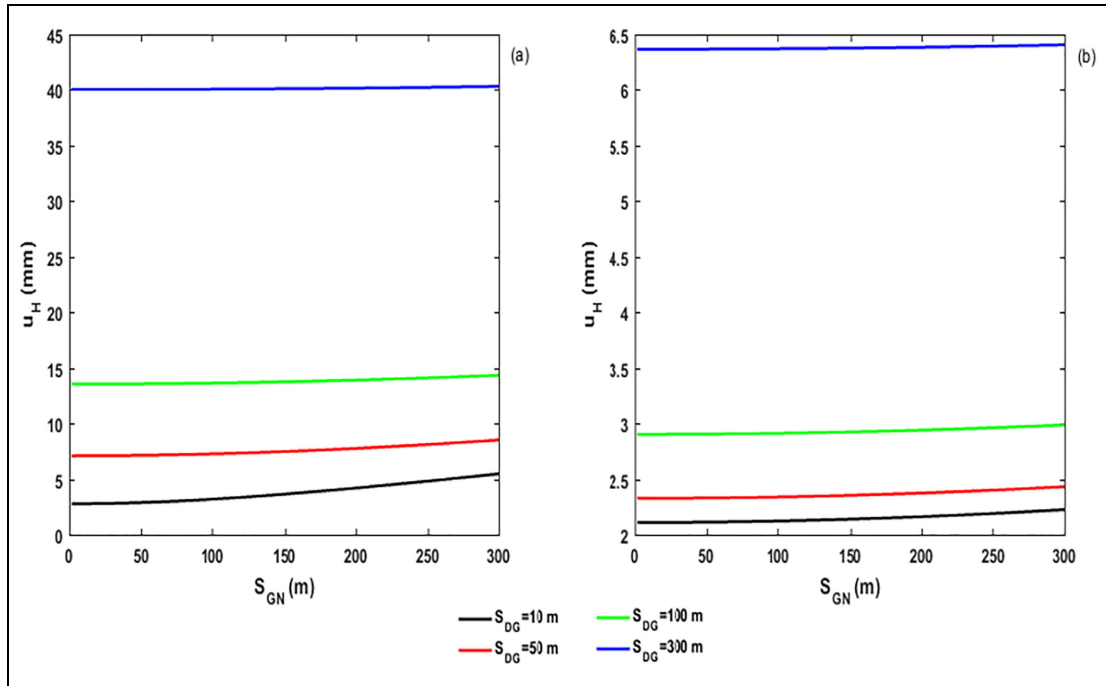


Figure 13. Strong influence of S_{DG} on overall uncertainty using Class T3 and T1 total stations respectively for figures (a) and (b), ($z_1 = 80gon$, $z_2 = 70gon$, $z_3 = 100gon$, $z_4 = 90gon$).

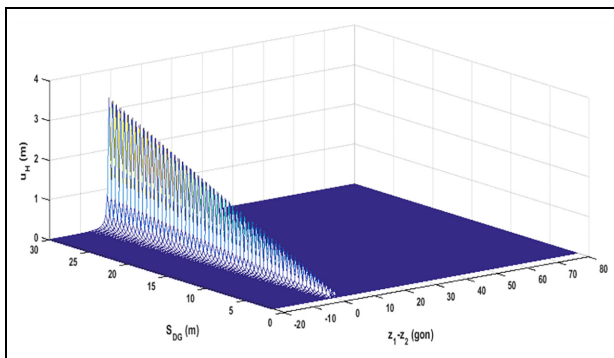


Figure 14. Variation of overall uncertainty as a function of S_{DG} and $z_1 - z_2$ for a class T3 total station. ($z_2 = 70gon$, $z_3 = 100gon$, $z_4 = 90gon$, $S_{GN} = 20m$).

the target point provided that small differences in zenith angles $z_1 - z_2$ are avoided. What's more, for small spans, the front-back measurement method for a distance $S_{DG} = 10m$, the front height of the prism has a relative contribution of 90% for a zenith angle difference $z_1 - z_2 = 40gon$.

Acknowledgements

The authors are grateful to the National Advanced School of Public Works (NASPW) for providing the ideal framework for the completion of this work. Moreover, this work is under the project sanctioned by the laboratory of topography modeling materials and methods of NASPW.


Declaration of conflicting interests

The author(s) declared no potential conflicts of interest with respect to the research, authorship, and/or publication of this article.

Funding

The author(s) received no financial support for the research, authorship, and/or publication of this article.

ORCID iD

Achille Germain Feumo  <https://orcid.org/0000-0002-2545-5373>

Data availability statement

The authors confirm that they have included data availability in our main manuscript file and the data will be made available on reasonable request. These data have been collected from a Swedish regulation called SIS-TS 21143: 2009 standard.

References

1. Idoje G, Dagiuklas T, and Igbal M. "survey for smart farming technologies challenges and issues" *Comp and Elect Eng* 2021; 92: 107104.
2. Hussein LY, Alwan IA and Ataiwe TN. Smart city 3D modeling with a total station and a smartphone. *IOP Conf Ser Earth Env Sci* 2023: 1129.
3. Harvey D. *Propagation of uncertainty-Chemistry Libre texts*. Greencastle, IN: Depauw University, 2020.

4. Cheng Z, Wang H, Han L, et al. An accurate orientation measurement system of self-propelled artillery barrel based on coordinate system mapping. *Meas Sci Technol* 2022; 33: 115003.
5. Zhou XP and Sun M. Study on accuracy measure of trigonometric leveling. *Appl Mech Mater* 2013; 329: 373–377.
6. Ghilani CD and Wolf PR (eds). *Adjustment computations: spatial data analysis*. 4th ed. Hoboken, New Jersey: John Wiley & Sons, Inc, 2006.
7. Zhuo Y. Measuring Inaccessible Points in Land Surveying and Analysis of their Uncertainty, the University of Gävle, 2012.
8. Kessel R, Kacker R and Berglund M. Coefficient of contribution to the combined standard uncertainty. *Metrologia* 2006; 43: S189–S195.
9. Trélat E. Contrôle optimal: théorie & applications, Vuibert, Collection “Mathématiques Concrètes,” 2005, p.246.
10. Duggal SK (ed.). *Remote elevation measurement (REM). Surveying*. 2nd ed. New Delhi: Tata McGraw-Hill Publishing Company Limited, 2004, p.593.
11. JCGM 100. Evaluation of measurement data – Guide to the expression of uncertainty in measurement. Joint Committee for Guides in Metrology (JCGM/WG 1), 2008.
12. Zhang RJ and Wang GJ. Sharp bounds on the approximation of a bézier polynomial by its quasi-control polygon. *Comput Aided Geom Des* 2006; 23: 1–16.
13. Ceylan A. Determination of the deflection of vertical components via GPS and leveling measurement: A case study of a GPS test network in Konya, Turkey. *Sci Res Essays* 2009; 4(12): 1438–1444.
14. Ghilani CD and Wolf PR (eds). *Adjustment computations: spatial data analysis*. 6th ed. Hoboken, New Jersey: John Wiley Sons, Inc, 2017.
15. Cederholm P and Jensen K. GPS measurement of inaccessible detail points. *Surv Rev* 2009; 41: 352–363.